Journal of Hazardous Materials 162 (2009) 688–694

Contents lists available at ScienceDirect

Journal of Hazardous Materials

journal homepage: www.elsevier.com/locate/jhazmat

Preparation and characterization of activated carbon from marine macro-algal biomass

R. Aravindhan, J. Raghava Rao*, B. Unni Nair

Chemical Laboratory, Central Leather Research Institute, Council of Scientific and Industrial Research, Adyar, Chennai 600020, India

ARTICLE INFO

Article history:
Received 7 January 2008
Received in revised form 25 April 2008
Accepted 20 May 2008
Available online 23 May 2008

Keywords:
Activated carbon
Macro-alga
Phenol adsorption
Column
Kinetics

ABSTRACT

Activated carbons prepared from two macro-algal biomass *Sargassum longifolium* (SL) and *Hypnea valentiae* (HV) have been examined for the removal of phenol from aqueous solution. The activated carbon has been prepared by zinc chloride activation. Experiments have been carried out at different activating agent/precursor ratio and carbonization temperature, which had significant effect on the pore structure of carbon. Developed activated carbon has been characterized by BET surface area (S_{BET}) analysis and iodine number. The carbons, ZSLC-800 and ZHVC-800, showed surface area around 802 and 783 $m^2\ g^{-1}$, respectively. The activated carbon developed showed substantial capability to adsorb phenol from aqueous solutions. The kinetic data were fitted to the models of pseudo-first-order, pseudo-second-order and intraparticle diffusion models. Column studies have also been carried out with ZSLC-800 activated carbon.

1. Introduction

Activated carbon widely finds use as adsorbent in gas and liquid phase separation, purification of gas and wastewater treatment. One of the most important fields where activated carbons with relatively higher surface area are needed is the water and wastewater treatment. Production of commercial activated carbons is still an expensive process. Hence the need of the hour is to screen for an alternative cost effective adsorbent. The utilization of innate materials available in huge quantities and the waste products from industrial or agricultural processes for wastewater treatment has been employed [1–7]. Agricultural byproducts are produced in huge quantities annually. More recently, potential of these materials for fabrication of activated carbon having properties on par with commercial activated carbon have been demonstrated [8–12]. Most of the agricultural byproducts produce high-purity chars with very adequate characteristics as precursors for activated carbon of high quality, useful in adsorption of gases and solutes from aqueous solutions [13,14]. Such carbon may have the potential to replace existing carbon, especially coal-based carbon used in many industrial applications.

Basically there are two different processes for the preparation of active carbon, viz. physical and chemical activation [15]. Physical activation involves the carbonization of a carbonaceous precursor followed by activation of the resulting char in the presence of some activating agents such as carbon dioxide or steam. Chemical activation, on the other hand, is a single step method of preparation of the precursor in the presence of chemical agents. In physical activation, the elimination of large amount of internal carbon mass is necessary to obtain a well developed carbon structure, whereas in chemical activation process all the chemical agents used are dehydrating agents that influence pyrolytic decomposition and inhibit formation of tar, thus enhancing the yield of carbon [15]. The chemicals used in the chemical activation are alkali (KOH, K_2CO_3, NaOH, and Na_2CO_3) and alkaline earth metals ($AlCl_3$ and $ZnCl_2$) and some acids (H_3PO_4 and H_2SO_4). In the case of chemical activation the effect of KOH and $ZnCl_2$ on the carbonization of precursors has been of particular interest and $ZnCl_2$ in particular is a widely used chemical agent in the preparation of activated carbon. Any cheap material with high carbon content and low inorganics can be used as a precursor for the production of activated carbon [16].

Phenols are the major organic constituents found in effluents of coal conversion processes, coke ovens, petroleum refineries, phenolic resin manufacturing, herbicide manufacturing, fiberglass manufacturing, tanning and petrochemicals. The terms “phenols” or “total phenols” or “phenolics” in wastewater treatment technology are used interchangeably either to denote simple phenol or a mixture of phenolic compounds in wastewater [17]. A wide range of phenolic compounds is toxic to microorganisms and inhibits nitrogen fixation. They have detrimental effect on the water quality and they are toxic to aquatic life. It has been reported that the toxicity of phenol varies with species, conditions of exposure and the

* Corresponding author. Tel.: +91 44 24411630; fax: +91 44 24911589.
E-mail address: rao_clri@yahoo.com (J. Raghava Rao).

0304-3894/$ – see front matter © 2008 Elsevier B.V. All rights reserved.
doi:10.1016/j.jhazmat.2008.05.083

duration of the tests. In addition, water containing phenolic compounds when used for irrigation caused retardation of plant growth. Phenolic compounds have long been recognized as one of the most recalcitrant and persistent substance because of the high toxicity of this compound [18]. In order to reduce the environmental load of harmful phenolic compounds, attention has to be focused on reducing the toxicity of wastewater by eliminating the discharge of these toxic substances or by making the discharges less harmful.

The objective of the present study is to evaluate the feasibility of macro-alga (seaweed) as a precursor for activated carbon production and employing the activated carbon thus prepared for the removal of phenol from aqueous solutions. The seaweed could be a promising raw material for the production of activated carbons because of their availability at low price. They can be used for the production of activated carbon with a high adsorption capacity, considerable mechanical strength and low ash content.

2. Materials and methods

2.1. Preparation of carbon

Beach-dried brown seaweed *Sargassum longifolium* (SL) and red seaweed *Hypnea valentiae* (HV) were procured from Central Salt and Marine Chemicals Research Institute (CSMCRI), Mandapam Camp, Ramnad District, India. The beach-dried seaweed was washed with distilled water and dried at $100 \pm 2\,^{\circ}C$ for 12 h. The dried material was then milled and sieved to uniform particle size (0.5 ± 0.1 mm) prior to activation process. Phenol and zinc chloride used were of analytical grade procured form Sd.Fine chemicals, India.

Twenty grams each of dried seaweed (SL and HV) were added to 200 mL of zinc chloride solution of desired concentration (10, 20, 30, 40, and 50%, w/v) and stirred for a period of 2 h. The excess zinc chloride solution was then decanted and the zinc treated seaweed (ZSL and ZHV) were then dried in an air oven for 24 h at $100 \pm 2\,^{\circ}C$. The ZSL and ZHV were then placed in a sealed ceramic crucible and kept in a muffle furnace. The temperature was ramped from room temperature to final temperatures of 400, 500, 600, 700 and $800\,^{\circ}C$ with a retention time of 2 h at a heating rate of $10\,^{\circ}C\,min^{-1}$. The resultant activated carbon (ZSLC and ZHVC) was washed with hot 0.5N HCl solution for 30 min to remove excess zinc chloride, filtered and rinsed with warm water until the washings were free of zinc ions. Then the ZSLC and ZHVC were dried in an air oven at $100 \pm 2\,^{\circ}C$ for 12 h and weighed to calculate the yield. The resultant carbons are referred to as ZSLC followed by the pyrolysis temperature throughout the manuscript, for example ZSLC-400 refers to the activated carbon pyrolysed at $400\,^{\circ}C$.

2.2. Preparation and analysis of phenol solutions

Stock solution of phenol was prepared by dissolving 1 g of phenol in 1 L of double distilled water. The stock solution was suitably diluted and used for adsorption experiments. The concentration of phenol was determined using a PerkinElmer Lambda 35 UV–vis Spectrophotometer at $\lambda_{max} = 270$ nm. Before making the measurements, the solutions were diluted to proper concentrations to give absorbances in the range of 0.1–1.2. The concentrations of the phenol solution were obtained from standard calibration curve.

2.3. Characterization of activated carbon

The yield of activated carbon is the % amount of activated carbon produced at the end of the activation step. This value indicates the activation process efficiency. Characterization of activated carbon was carried out by nitrogen adsorption–desorption isotherms recorded at $-196\,^{\circ}C$ using Sorptomatic 1990 analyzer. Prior to analysis the samples were out gassed in the analyzer degas port for 2 h at $100\,^{\circ}C$. The specific surface area S_{BET} was calculated using the standard Brunauer–Emmet–Teller (BET) method [19]. Iodine number defined as the mg of iodine per gram of carbon was determined by ASTM D 4607–86 method. The residual phenol concentration was then measured using PerkinElmer Lambda 35 UV–vis spectrophotometer by modified Folin phenol Ciocalteu method [20].

The thermal behavior of SL, HV, ZSL and ZHV was evaluated by using thermogravimetric analysis using NETZSCH STA 409C, thermal analyzer under nitrogen gas flow ($50\,mL\,min^{-1}$) at a heating rate of $20\,^{\circ}C\,min^{-1}$. The pH_{pzc} indicates the acid or basic character of the carbon surface [21]. The point of zero charge was determined from acid–base titration [22]. Fifty milliliters of 0.01 M NaCl solution was taken in different flasks. When the pH value was constant, 0.10 g of carbon sample was added to each flask and it was shaken for 24 h. The pH_{pzc} value is the point where the curve pH_{final} vs. $pH_{initial}$ crosses the line $pH_{initial} = pH_{final}$.

Determinations of C, H, N and S were performed in a CHN 1000 Leco, and FISONS EA1108 elemental analyzers. The proximate analysis was performed using gravimetric methods, the moisture content was calculated by weight difference employing a furnace and heating the sample for 2 h. The production of ash was estimated by heating the sample at $550\,^{\circ}C$ in a muffle furnace for 2 h until no mass variation was observed. The volatile matter was obtained by the standard procedure and the fixed carbon was determined by subtracting the percentages of moisture, volatile matter and ash from the sample [23–25].

2.4. Adsorption experiments

Batch adsorption experiments were carried out by employing known amount of ZSLC-800 and ZHVC-800. Phenol was used as the adsorbate in this investigation. The carbon dosage was varied from 1 to $10\,g\,L^{-1}$ and the initial phenol concentration was maintained at $100\,mg\,L^{-1}$, pH was adjusted to be 3.0 ± 0.2 and the experiments were conducted at $32 \pm 2\,^{\circ}C$. 50 mL of phenol solution was used for the experiments. The adsorption equilibrium for the adsorption of phenol was attained at around 4 h with ZSLC-800 and 5 h with ZHVC-800. The kinetic studies were carried out by contacting $10\,g\,L^{-1}$ of activated carbon with varying concentrations of phenol solution ($50–200\,mg\,L^{-1}$). The bottles were placed in a temperature controlled mechanical shaker at $32 \pm 2\,^{\circ}C$ and was agitated at a speed of 75 strokes/min. The samples were withdrawn at known time intervals to study the kinetics of the adsorption process. Samples were filtered through a 0.45 μm pore size cellulose acetate membrane filter and then analyzed for the supernatant phenol concentration using PerkinElmer Lambda 35 UV–vis Spectrophotometer at $\lambda_{max} = 270$ nm. The amount of phenol adsorbed on to the activated carbon at equilibrium was calculated from the mass balance of the equation as given below:

$$q_e = (C_0 - C_e)\frac{V}{W} \quad (1)$$

where C_0 and C_e are the initial and equilibrium concentration of phenol solution ($mg\,L^{-1}$), respectively, q_e the equilibrium phenol concentration on seaweed ($mg\,g^{-1}$), V the volume of the phenol solution (L) and W is the mass of the carbon used (g). The experiments were done in duplicate.

2.5. Column studies

A glass column of 30 cm height and 1.8 cm internal diameter was used to carry out the column studies. Activated carbon prepared from *S. longifolium* (ZSLC-800) was employed for the column

studies. The column was packed with ZSLC-800. The adsorbate solution was pumped upflow through the bed using a peristaltic pump. Experiments were carried out at varying flow rate (5, 10 and 15 mL min^{-1}) and packed bed height (5, 10, and 15 cm) employing phenol solution of initial concentration 50 mg L^{-1}. Samples were filtered through a 0.45 μm pore size cellulose acetate membrane filter and then analyzed for the supernatant phenol concentration using PerkinElmer Lambda 35 UV–vis Spectrophotometer at λ_{max} = 270 nm.

3. Results and discussions

Two abundantly available seaweeds namely *S. longifolium* (SL) and *H. valentiae* (HV) have been utilized as precursors for the production of activated carbon. The proximate analysis of SL yielded; moisture 8.75%, fixed carbon 34.45%, volatile matter 51.65% and ash 5.15%. The proximate analysis of HV yielded; moisture 8.19%, fixed carbon of 30.04%, volatile matter 55.48% and ash 6.30%. A two-step method has been adopted for the preparation of activated carbon, wherein the first step involves the treatment of seaweed with zinc chloride solution for 2 h, followed by drying at dried at 100 ± 2 °C for 24 h. The second step involves the pyrolysis at higher temperature.

3.1. Effect of activating agent

The % yield was used as a parameter to choose the optimum quantity of the zinc chloride required for impregnating the seaweed. An additional experiment was carried out without the impregnation of seaweeds with $ZnCl_2$. The results of these experiments are provided in Table 1. It is observed that $ZnCl_2$ impregnation has significant effect on improving the % yield of activated carbon. Pyrolysis of SL and HV without $ZnCl_2$ impregnation resulted in relatively low yield of 12.24 and 13.58%, respectively, because a large amount of carbon was removed as CO, CO_2 CH_4, aldehydes and distillation of tar [26]. Also, it has been observed from the table that with an increase in the quantity of zinc chloride from 10 to 30%, the product yield increased from 27.35 to 32.42% and 28.79 to 33.65% for ZSLC-600 and ZHVC-600, respectively. This increase in product yield was observed up to certain concentration. This could be attributed to the fact that $ZnCl_2$ selectively stripped H and O away from the seaweed as H_2O and H_2 rather than hydrocarbons, CO and CO_2 [27]. Subsequent increase in the quantity of zinc chloride to 50% decreased the % product yield to 22.12 and 21.17%, respectively for ZSLC-600 and ZHVC-600. This could be attributed to enhancement of carbon burning-off by extra $ZnCl_2$ [26]. This property inhibits the formation of tars and any other liquids that can clog up the pores of the sample. Also, because of zinc chloride impregnation, the movement of volatiles through the pore passages will not be hindered and so will be subsequently released from the carbon surface during activation. Hence, subsequent increase in impregnation ratio increases the release of volatiles from the sample and therefore decreases the yield of the activated carbon. A similar trend has been observed for both the materials. In both the experiments, since the % yield of carbon was high at 30% offer of zinc chloride, the precursors have been pretreated with 30% $ZnCl_2$ for a period of 2 h prior to pyrolysis.

Table 1
Effect of quantity of activating agent added on the % yield of activated carbon

Activating agent ($ZnCl_2$) (%)	Yield (%)	
	ZSLC-600	ZHVC-600
0	12.24	13.58
10	27.35	28.79
20	29.14	29.87
30	32.42	33.65
40	25.15	26.16
50	21.17	22.12

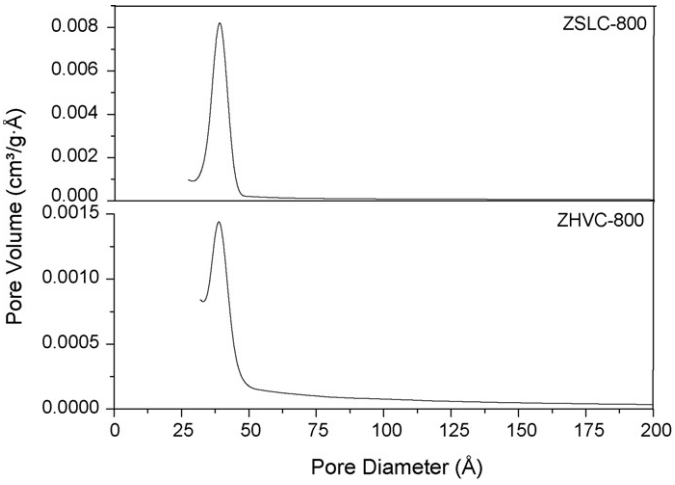

Fig. 1. Pore size distribution of activated carbons ZSLC-800 and ZHVC-800 by BJH method.

3.2. Effect of pyrolysis temperature

The temperature of pyrolysis is yet another vital parameter which affects the physical characteristics of the activated carbon. The % yield obtained by varying the pyrolysis temperature for the preparation of activated carbon from SL and HV are provided in Table 2. It is observed from the table that, the % yield of carbon decreased with the increase in pyrolysis temperature. This is expected because, at a higher temperature more volatiles are released, resulting in the lower % yield. The effects of activation temperature on the apparent density and porosity of the activated carbon are also shown in Table 2. The BET surface area (S_{BET}) increased from 511 to 802 cm^2 g^{-1} and 498 to 783 cm^2 g^{-1} with the increase in activation temperature from 400 to 800 °C for zinc pretreated SL and HV, respectively. The iodine number, which is the measure of activity level (higher number indicates higher degree of activation) increased with increase in activation temperature. The iodine number increased from 489 to 1041 mg g^{-1} and 459 to 962 mg g^{-1} as the activation temperature increased from 400 to 800 for zinc treated SL and HV, respectively.

The BET surface area, microporous surface area, total pore volume, micropore volume and the average pore diameter of the activated carbon prepared in this work are provided in Table 3. It is observed that the activated carbon prepared from both the seaweed have a high surface area, which is primarily attributed to the meso- and macro-pore, as the % contribution of micropore is only 17.4 and 16.2% of the BET surface area for ZSLC-800 and ZHVC-800, respectively. This is supported by the pore size distribution of the carbons determined using the BJH method as shown in Fig. 1. The average pore diameter of 39 and 36 Å has been obtained for ZSLC-800 and ZHVC-800, respectively. Also, the pH of the carbon is around 7.9 ± 0.3 and the pH_{pzc} was determined to be 4.85 and 4.72 for ZSLC-800 and ZHVC-800, respectively. Thus, it could be inferred that the prepared carbon is less acidic in nature.

3.3. Thermogravimetric analysis (TGA)

Thermograms obtained from the thermogravimetric (TG) analysis of the untreated as well as zinc chloride treated SL is shown in Fig. 2. The loss of weight during the TG analysis of raw SL can

Table 2
Effect of pyrolysis temperature on the % yield, S_{BET}, iodine number, apparent density of activated carbons

Temperature (°C)	ZSLC-800				ZHVC-800			
	Yield (%)	S_{BET} ($m^2\,g^{-1}$)	Iodine number ($mg\,g^{-1}$)	App. density ($g\,mL^{-1}$)	Yield (%)	S_{BET} ($m^2\,g^{-1}$)	Iodine number ($mg\,g^{-1}$)	App. density ($g\,mL^{-1}$)
400	44.15	511	489	0.92	43.25	498	459	0.97
500	42.71	550	534	0.82	40.62	552	574	0.90
600	32.72	622	597	0.75	31.14	612	588	0.91
700	31.91	720	757	0.67	29.17	712	677	0.75
800	30.75	802	1041	0.65	28.67	783	962	0.69

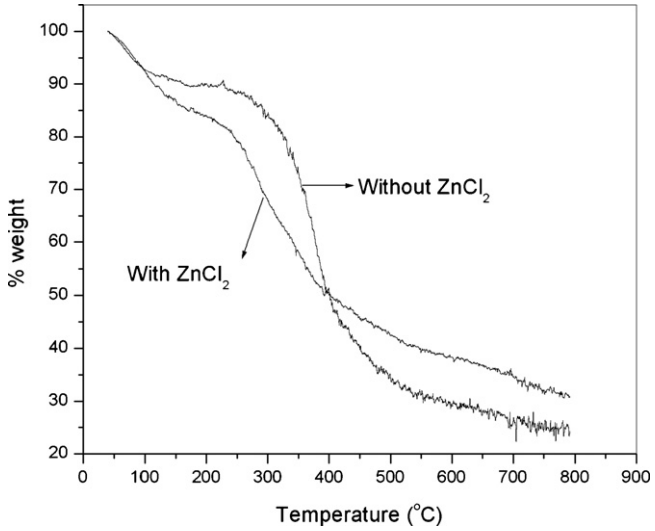

Fig. 2. Thermogravimetric (TG) analysis of the raw as well as zinc chloride treated *Sargassum longifolium*.

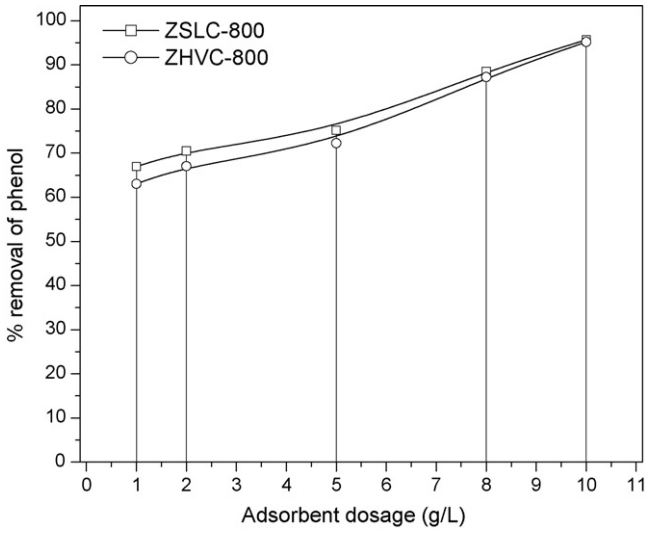

Fig. 3. Effect of adsorbent dosage on the phenol removal at an initial phenol concentration of 100 mg L^{-1} and pH of 3.0 ± 0.1.

be divided in to three stages. The first weight loss (~10.20%) by heating the materials upto 150 °C has been due to the moisture elimination. The second stage of 150–450 °C corresponds to primary carbonization, which has a major weight loss (52.26%). This stage presents a considerably greater weight loss for the untreated seaweed due to the elimination of volatile matters and tars. The zinc chloride pretreatment as expected caused a partial carbonization of the seaweed and the weight loss variation curve for the zinc treated material shows a slight and continuous decrease when compared to the untreated seaweed. Since $ZnCl_2$ undergoes little weight loss at these temperatures, the observed weight loss was only for seaweed [28]. This loss of weight is lower than that obtained by untreated seaweed. Thus, the presence of $ZnCl_2$ has a significant effect on the pyrolysis behavior of the seaweed residue. The third stage in the 450–800 °C range indicates the decomposition of a structure with higher stability [27]. Above 800 °C, the weight loss was small thus indicating that the basic structure of the char has been formed approximately at this temperature. A similar trend was observed for HV seaweed.

3.4. Adsorption of phenol

The activated carbons ZSLC-800 and ZHVC-800, prepared in this study have been tested for their phenol adsorption capacity. The removal of phenol increased with an increase in the carbon dosage from 1 to 10 g L^{-1}. The increase in adsorption of phenol with an increase in carbon dosage can be attributed to the availability of larger surface area and more adsorption sites. The effect of carbon dosage on the phenol removal efficiency has been provided in Fig. 3. It is observed that the % phenol removal by ZSLC-800 increased from 67 to 96% and for ZHVC-800 the % phenol removal increased from 63 to 95% with an increase in adsorbent dosage.

3.5. Adsorption kinetics

The kinetics of adsorption describes the rate of uptake of phenol on to the activated carbon and this rate controls the equilibrium time. It has been observed that 70–80% of the adsorption process takes place within 1 h of experiment. The kinetics of phenol

Table 3
Characteristics of prepared activated carbon

Sample	Iodine number ($mg\,g^{-1}$)	S_{BET}[a] ($m^2\,g^{-1}$)	S_M[b] ($m^2\,g^{-1}$)	V_T[c]	V_M[d]	D_p[e] (Å)
ZSLC-800	1041	802	140	0.517	0.351	39
ZHVC-800	962	783	127	0.481	0.211	36

[a] S_{BET}, BET surface area.
[b] S_M, micropore area.
[c] V_T, total pore volume.
[d] V_M, micropore volume.
[e] D_p, average pore diameter.

Table 4
Rate constants for kinetic models at various initial concentrations of phenol

Carbon type	Initial conc. ($mg\,L^{-1}$)	$q_{e(exp)}$ ($mg\,g^{-1}$)	First-order rate constants			Pseudo-second-order rate constants			Intraparticle diffusion constants	
			k_1 (min^{-1})	$q_{e\,(cal)}$ ($mg\,g^{-1}$)	R^2	k_2 ($g\,mg^{-1}\,min^{-1}$)	$q_{e\,(cal)}$ ($mg\,g^{-1}$)	R^2	k_p ($mg\,g^{-1}\,min^{-1/2}$)	R^2
ZSLC-800	50	9.84	0.0143	2.650	0.988	0.0178	9.98	0.999	0.2051	0.946
	75	12.64	0.0127	5.790	0.988	0.0060	13.03	0.996	0.4239	0.988
	100	14.48	0.0187	7.080	0.989	0.0063	15.06	0.999	0.5361	0.903
	150	21.48	0.0161	18.770	0.891	0.0012	23.87	0.997	1.2193	0.989
	200	24.64	0.0123	17.090	0.948	0.0015	26.80	0.993	1.3182	0.952
ZHVC-800	50	9.86	0.0142	2.355	0.989	0.0204	9.98	0.999	0.1836	0.946
	75	12.89	0.0127	5.167	0.989	0.0072	13.21	0.997	0.3791	0.988
	100	15.07	0.0182	6.307	0.988	0.0077	15.53	0.999	0.4798	0.903
	150	22.38	0.0161	18.770	0.891	0.0016	23.96	0.986	1.0905	0.989
	200	26.26	0.0123	17.080	0.948	0.0020	27.75	0.995	1.1792	0.952

removal by the seaweed-based activated carbons ZSLC-800 and ZHVC-800 have been analyzed by pseudo-first-order and pseudo-second-order kinetic equation at different initial concentrations of phenol. The experimental data and the calculated data along with the kinetic constants are provided in Table 4 and have been compared based on the regression coefficient (R^2).

The rate constant of adsorption is determined from the following pseudo-first-order rate expression given by Langergren [29]:

$$\log(q_e - q) = \frac{\log q_e - k_1 t}{2.303} \quad (2)$$

where q_e is the amount of phenol adsorbed ($mg\,g^{-1}$) at equilibrium, q is the amount of phenol adsorbed ($mg\,g^{-1}$) at time t (min), k_1 is the pseudo-first-order rate constant of adsorption. A straight line of $\log(q_e - q)$ vs. t suggests the applicability of this kinetic model. The first-order rate constant (k_1) and q_e were determined from the slopes and intercepts of plots of $\log(q_e - q)$ vs. t at different adsorbent dosages.

The kinetics of adsorption can also be described by pseudo-second-order equation and it is given by the equation [30]:

$$\frac{t}{q} = \frac{1}{k_2 q_e^2} + \frac{t}{q_e} \quad (3)$$

The second-order rate constant (k_2) and q_e were determined from the slope and intercepts of the plots obtained by plotting $tq_t{}^{-1}$ vs. time t. The correlation coefficients for the first-order kinetic model were determined and compared with that of second-order kinetic model. It is seen that the correlation coefficient of first-order kinetic are lower than in the case of second-order kinetic model for both ZSLC-800 and ZHVC-800. This shows that kinetics of phenol adsorption by the seaweed-based activated carbons is better described by pseudo-second-order kinetic model rather than pseudo-first-order kinetic model. The linearity of the plot (figure not shown) also shows the applicability of the pseudo-second-order kinetic model, which has average regression coefficient (R^2) of 0.997. Also, $q_{e(cal)}$ using pseudo-second-order kinetic model is on par with $q_{e(exp)}$ which has been obtained experimentally.

The data were further processed for testing the role of diffusion (as a rate-controlling step) in the adsorption process. According to the Morris and Weber [31] model, uptake is proportional to the square root of contact time during the course of adsorption. Accordingly

$$q_t = k_d \sqrt{t} \quad (4)$$

k_d is the rate constant of intraparticle transport ($mg\,g^{-1}\,min^{-1/2}$).

Plot of uptake q_t vs. $\sqrt{t}$ should be linear if intraparticle diffusion is involved in the adsorption process and if the lines pass through the origin then intraparticle diffusion is the rate-controlling step. However, in the present adsorption process, intraparticle diffusion is involved but is not the rate limiting mechanism, as the lines did not pass through the origin.

3.6. Analysis of column data

The total quantity of phenol adsorbed in the column (P_{ad}) is calculated from the area below the breakthrough curve (outlet phenol concentration vs. time) multiplied by the flow rate. By dividing P_{ad} by the biosorbent mass (M) the uptake capacity (Q) of the biomass can be obtained [32].

The breakthrough time (t_b) (the time at which phenol concentration in the effluent reached >1 $mg\,L^{-1}$) and bed exhaustion time (t_e, the time at which phenol concentration in the effluent exceeded 99 $mg\,L^{-1}$) were used to evaluate the overall adsorption zone (Δt) as follows [33]:

$$\Delta t = t_e - t_b \quad (5)$$

The length of the mass transfer zone (Z_m), also called as critical bed length, can be calculated from the breakthrough curve as follows [33]:

$$Z_m = Z\left(1 - \left(\frac{t_b}{t_e}\right)\right) \quad (6)$$

where Z is the bed height (cm).

Effluent volume (V_{eff}) can be calculated as follows [32]:

$$V_{eff} = Ft_e \quad (7)$$

where F is the volumetric flow rate ($mL\,min^{-1}$).

Total amount of phenol sent to column (P_{total}) can be calculated as follows [32]:

$$P_{total} = \frac{C_0 F t_e}{1000} \quad (8)$$

The % removal of phenol with respect to flow volume can be calculated as follows [32]:

$$\text{phenol removal}\,(\%) = \left(\frac{P_{ad}}{P_{total}}\right) \times 100 \quad (9)$$

3.7. Effect of flow rate

Flow rate is one of the important characteristics in evaluating sorbents for continuous-treatment of phenol containing effluents on an industrial scale [34]. The effect of flow rate on phenol adsorption by ZSLC was studied by varying the flow rate from 5 to 15 $mL\,min^{-1}$, while the bed height and initial phenol concentration were held constant at 15 cm and 100 $mg\,L^{-1}$, respectively. The plots of effluent phenol concentration vs. time at different flow rates are shown in Fig. 4. All the calculated parameters are provided in Table 5. An earlier breakthrough and exhaustion time

Table 5
Column data and parameters obtained at different bed heights and different flow rates with initial phenol concentration of 100 mg L^{-1}

Bed height (cm)	Flow rate (mL min^{-1})	Uptake (mg g^{-1})	t_b (h)	t_e (h)	Δt (h)	T_s (h)	dc/dt (mg L^{-1} h^{-1})	V_{eff} (L)	Z (cm)	Z_m (cm)	Total phenol removal (%)
5	5	68.21	8	22.5	14.5	7.73	4.39	6.75	5	3.22	34.36
10	5	66.35	13.5	37	23.5	15.04	2.81	11.1	10	6.35	40.65
15	5	58.03	22	45	23	19.38	2.2	13.5	15	7.67	43.84
15	10	62.06	10	31	21	10.55	4.05	18.6	15	10.16	34.03
15	15	73.32	5	25	20	8.32	8.66	22.5	15	12.00	33.24

were observed in the profile, when the flow rate was increased to 15 mL min^{-1}. The flow rate also strongly influenced the phenol uptake capacity of ZSLC-800. The uptake capacity was 58.03, 62.06 and 73.32 mg g^{-1}, for a flow rate of 5, 10 and 15 mL min^{-1}, respectively. The total phenol removal percentage was actually recorded as 43.84, 34.03 and 33.24% at 5, 10 and 15 mL min^{-1}, respectively. Successful design of a column adsorption process required prediction of the concentration–time profile or breakthrough curve for the effluent [35]. Various mathematical models can be used to describe fixed bed adsorption. Among these, the Thomas model is simple and widely used by several investigators [32,35]. The linearized form of Thomas model is expressed as follows:

$$\ln\left(\frac{C_0}{C}-1\right)=\left(\frac{k_{Th}Q_0M}{F}\right)-\left(\frac{k_{Th}C_0V}{F}\right) \quad (10)$$

where k_{Th} is the Thomas model constant (L mg^{-1} h^{-1}), Q_0 the maximum solid-phase concentration of solute (mg g^{-1}), V the throughput volume (L). The model constants k_{Th} and Q_0 can be determined from a plot of $\ln((C_0/C)-1)$ vs. t at a given flow rate [32]. The model gave a good fit of the experimental data at all flow rates examined with high correlation coefficients greater than 0.978. The values of k_{Th} obtained from Thomas model were 0.0052, 0.0042 and 0.0047 L mg^{-1} h at 5, 10 and 15 mL min^{-1}, respectively. The values of Q_0 obtained from the Thomas model were 37.34, 89.09 and 95.82 mg g^{-1} at 5, 10 and 15 mL min^{-1}, respectively.

3.8. Effect of bed height

Accumulation of phenol in the packed bed column is largely dependent on the quantity of sorbent inside the column. The adsorption breakthrough curves obtained by varying the bed heights from 5 to 15 cm at 5 mL min^{-1} flow rate and 100 mg L^{-1} initial phenol concentration for ZSLC-800 are given in Fig. 5. In order to yield different bed heights, 3.40, 6.80 and 10.2 g of ZSLC-800 were added to produce a bed height of 5, 10 and 15 cm, respectively. All the calculated parameters are given in Table 5. Both breakthrough time and exhaustion time increased with increasing bed height and resulted in a broadened mass transfer zone, as more binding sites are available for adsorption. The slope of the S-curve from t_b to t_e (dc/dt) decreased as the bed height increased from 5 to 15 cm, indicating the breakthrough curve becomes steeper and the mass transfer zone (Δt) becomes shorter as the bed height decreased (Fig. 5). The percentage removal of phenol was significantly affected by bed height, as 34.36 increased to 43.84% when the bed height increased from 5 to 15 cm. This trend was expected because uptake capacity usually depends on the amount of sorbent available for adsorption. Also, a significant increasing trend was observed for total phenol removal percentages as 34.36, 40.65 and 43.84% for 5, 10 and 15 cm, respectively.

BDST is a simple model, which states that bed height (Z) and service time (t) of a column bears a linear relationship. The equation can be expressed as [36] follows:

$$t=\left(\frac{N_0Z}{C_0\upsilon}\right)-\left(\frac{1}{k_aC_0}\right)\ln\left(\frac{C_0}{C_b}-1\right) \quad (11)$$

where C_b is the breakthrough sorbate concentration (mg L^{-1}), N_0 the adsorption capacity of bed (mg L^{-1}), υ the linear velocity (cm h^{-1}), and k_a is the rate constant (L mg^{-1} h^{-1}). The column service time was selected as time when the effluent phenol concentration reached >1 mg L^{-1}. The plot of service time against bed height at a flow rate of 5 mL min^{-1} was linear (R^2 = 0.973) indicating the validity of BDST model for the present system. The adsorption capacity of the bed per unit bed volume, N_0, was calculated from the slope of BDST plot, assuming initial concentration, C_0 and linear velocity υ, as constant during the column operation. The rate constant, k_a, calculated from the intercept of BDST plot,

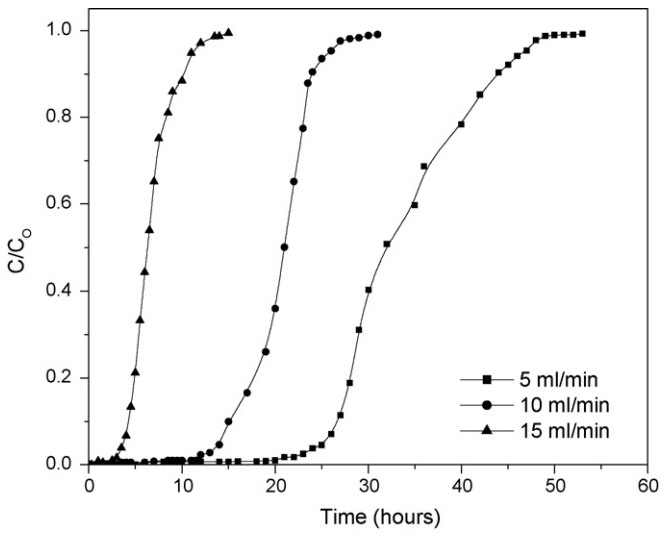

Fig. 4. Effect of flow rates on packed-bed for ZSLC-800.

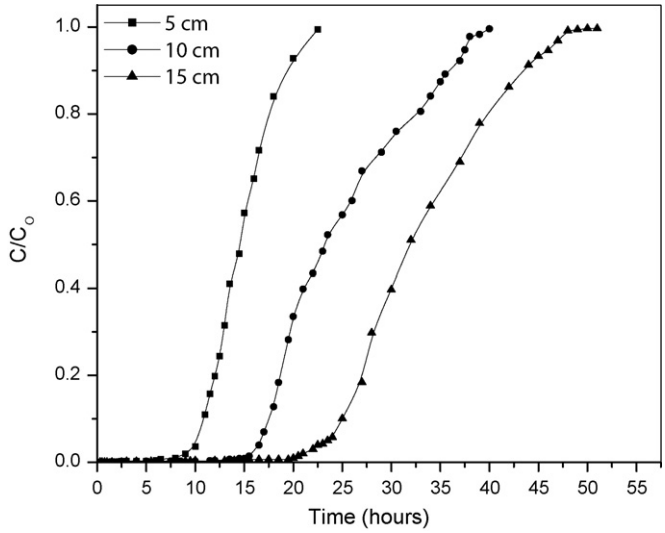

Fig. 5. Effect of bed heights on packed-bed for ZSLC-800.

characterizes the rate of solute transfer from the fluid phase to the solid phase [37]. The computed N_0 and k_a were 26.32 mg mL^{-1} and 0.0037 L mg^{-1} h^{-1}, respectively. If k_a is large, even a short bed will avoid breakthrough, but as k_a decreases a progressively longer bed is required to avoid breakthrough [37]. The BDST model parameters can be useful to scale up the process for other flow rates without further experimental run.

4. Conclusions

In the present study, activated carbons containing high surface area have been prepared from two commonly available seaweed, viz. *S. longifolium* and *H. valentiae* by employing $ZnCl_2$ as an activating agent. The best conditions for the production of high surface area activated carbon are; activation using 30% $ZnCl_2$, carbonization time of 2 h and carbonization temperature of 800 °C. At this optimal condition, the BET surface area of 802 and 783 m^2 g^{-1} and iodine number of 1041 and 961 mg g^{-1} have been obtained for ZSLC-800 and ZHVC-800, respectively. The adsorption experiments indicate that the activated carbon from seaweed has good adsorption capacity for phenol from aqueous solutions. A comparison of the kinetic models of the overall adsorption rate showed that the pseudo-second-order rate model best describes the adsorption of phenol by activated carbon. Thomas model for different flow rate and BDST model for different column bed heights have been employed. The model constants belonging to each model have been determined by linear regression techniques and are proposed for the use in column design. To sum up, the easy availability and suitability for the production of activated carbon, makes SL and HV a potential and low cost natural materials for the production of activated carbon.

Acknowledgements

One of the authors (R.A.) is grateful to Council of Scientific and Industrial Research, Government of India, New Delhi for granting Research Associateship (RA) for his Ph.D. program.

References

[1] W.E. Marshall, E.T. Champagne, Agricultural by-product as adsorbents for metal ions in laboratory prepared solutions and manufacturing wastewaters, J. Environ. Sci. Health A 30 (1995) 241–261.
[2] C. Namasivayam, K. Kadirvelu, Activated carbon from coirpith by physical and chemical activation methods, Bioresour. Technol. 62 (1997) 123–127.
[3] E.A. Oliveira, S.F. Montanher, A.D. Andrade, J.A. Nóbrega, M.C. Rollemberg, Equilibrium studies for the sorption of chromium and nickel from aqueous solutions using raw rice bran, Proc. Biochem. 40 (2005) 3485–3490.
[4] Y. Orhan, H. Buyukgugor, The removal of heavy metals by using agricultural wastes, Water Sci. Technol. 28 (1993) 247–255.
[5] R. Aravindhan, B. Madhan, J.R. Rao, B.U. Nair, Recovery and reuse of chromium from tannery wastewaters using *Turbinaria ornato* seaweed, J. Chem. Technol. Biotechnol. 79 (2004) 1251–1258.
[6] R. Aravindhan, J.R. Rao, B.U. Nair, Removal of basic yellow dye from aqueous solution by sorption on green alga *Caulerpa scalpelliformis*, J. Hazard. Mater. 142 (2007) 68–76.
[7] N.N. Fathima, R. Aravindhan, J.R. Rao, B.U. Nair, Solid waste removes toxic liquid waste: adsorption of chromium(VI) by iron complexed protein waste, Environ. Sci. Technol. 39 (2005) 2804–2810.
[8] K. Gergova, N. Petrov, S. Eser, Adsorption properties and microstructure of activated carbons produced from agricultural by-products by steam pyrolysis, Carbon 32 (1994) 693–702.
[9] K. Kadirvelu, B. Brasquet, P. Le Cloirec, Removal of Cu(II) Pb(II) and Ni(II) by adsorption onto activated carbon cloth, Langmuir 16 (2000) 8404–8409.
[10] C. Namasivayam, K. Kadirvelu, Agricultural solid waste for the removal of heavy metals: adsorption of Cu(II) by coirpith carbon, Chemosphere 34 (1997) 377–399.
[11] A.E. Sikaily, A.E. Nemr, A. Khaled, O. Abdelwehab, Removal of toxic chromium from wastewater using green alga *Ulva lactuca* and its activated carbon, J. Hazard. Mater. 148 (2007) 216–228.
[12] S.J.T. Pollard, F.E. Thompson, G.L. McConnachie, Microporous carbons from *Moringa oleifera* husks for water purification in less developed countries, Water Res. 29 (1995) 337–347.
[13] S. Ismadji, Y. Sudaryanto, S.B. Hartono, L.E.K. Setiawan, A. Ayucitra, Activated carbon from char obtained from vacuum pyrolysis of teak sawdust: pore structure development and characterization, Bioresour. Technol. 96 (2005) 1364–1369.
[14] F.R. Reinoso, M.M. Sabio, Activated carbons from lignocellulosic materials by chemical and/or physical activation: an overview, Carbon 30 (1992) 1111–1118.
[15] R.C. Bansal, J.B. Donnet, F. Stoeckli, Active Carbon, Dekker, New York, 1988.
[16] W.T. Tsai, C.Y. Chang, S.L. Lee, Preparation and characterization of activated carbons from corn cob, Carbon 35 (1997) 1198–1200.
[17] S. Beszedits, M.D. Silbert, Treatment of Phenolic Wastewaters, B&L Information Services, Toronto, 1990, ISBN 0-920720-26-9.
[18] Canadian Environmental Protection Act (CEPA) Priority Substances List Assessment Report: Phenol, 1999.
[19] S. Brunauer, P.H. Emmett, E. Teller, Adsorption of gases in multimolecular layers, J. Am. Chem. Soc. 60 (1938) 309–319.
[20] L.S. Clesceri, A.E. Grenberg, A.D. Eaton, Standard Methods for the Examination of Water and Wastewater, 20th ed., American Public Health Association, USA, 1998, pp. 574–585.
[21] J.S. Noh, J.A. Schwarz, Estimation of the point of zero charge of simple oxides by mass titration, Colloid Interf. Sci. 130 (1989) 157.
[22] J. Rivera-Utrilla, I. Bautista-Toledo, M.A. Ferro-García, C. Moreno-Castilla, J. Chem. Technol. Biotechnol. 76 (2001) 1209.
[23] E.W. Crampton, L.A. Maynard, The relation of cellulose and lignin content to the nutritive value animal feeds, J. Nutr. 15 (1938) 383–395.
[24] IS 1350, Part I. Methods of Test for Coal and Coke, Proximate Analysis. Bureau of Indian Standards, Manak Bhawan, New Delhi, India, 1984.
[25] IS 355. Methods for the determination of Chemical Composition of Ash of Coal and Coke. Bureau of Indian Standards. Manak Bhawan, New Delhi, India, 1984.
[26] Q. Qian, M. Machidaand, H. Tatsumoto, Preparation of activated carbons from cattle-manure compost by zinc chloride activation, Bioresour. Technol. 98 (2007) 353–360.
[27] F. Caturla, M. Molina-Sabio, F. Rodriguez-Reinoso, Preparation of activated carbon by chemical activation with $ZnCl_2$, Carbon 29 (1991) 999–1007.
[28] I.I. Salame, T.J. Bandosz, Role of surface chemistry in adsorption of phenol on activated carbons, J. Colloid Interf. Sci. 264 (2003) 307–312.
[29] S. Lagergren, Zur theorie der sogenannten adsorption gelöster stoffe. Kungliga Svenska Vetenskapsakademiens, 24, Handlingar, 1898, pp. 1–39.
[30] Y.S. Ho, G. McKay, Pseudo-second-order model for sorption processes, Proc. Biochem. 34 (1999) 4510–5465.
[31] W.J. Weber, J. Morris, Kinetics of adsorption on carbon from solution, J. Saint Eng. Div. Am. Soc. Civ. Eng. 89 (1963) 31–39.
[32] Z. Aksu, F. Gonen, Biosorption of phenol by immobilized activated sludge in a continuous packed bed: prediction of breakthrough curves, Proc. Biochem. 39 (2003) 599–613.
[33] B. Volesky, J. Weber, J.M. Park, Continuous-flow metal biosorption in a regenerable *Sargassum* column, Water Res. 37 (2003) 297–306.
[34] M. Zhao, J.R. Duncan, R.P. Van Hille, Removal and recovery of zinc from solution and electroplating effluent using *Azolla filiculoides*, Water Res. 33 (1999) 1516–1522.
[35] G. Yan, T. Viraraghavan, Heavy metal removal in a biosorption column by immobilized *M. rouxii* biomass, Bioresour. Technol. 78 (2001) 243–249.
[36] R.A. Hutchins, New method simplifies design of activated carbon systems, Chem. Eng. 80 (1973) 133–138.
[37] D.O. Cooney, Adsorption Design for Wastewater Treatment, CRC Press, Boca Raton, 1999.